Membrane vibration analysis above the Nyquist limit with fluorescence videogrammetry

Adrian A. Dorrington
National Research Council Associate
Advanced Sensing and Optical Measurement Branch
Mail Stop 236, NASA Langley Research Center, Hampton, VA 23681

Thomas W. Jones, Paul M. Danehy
Advanced Sensing and Optical Measurement Branch
Mail Stop 236, NASA Langley Research Center, Hampton, VA 23681

Richard S. Pappa‡.
Structural Dynamics Branch
Mail Stop 230, NASA Langley Research Center, Hampton, VA 23681

ABSTRACT

A new method for generating photogrammetric targets by projecting an array of laser beams onto a membrane doped with fluorescent laser dye has recently been developed. In this paper we review this new fluorescence based technique, then proceed to show how it can be used for dynamic measurements, and how a short pulsed (10 ns) laser allows the measurement of vibration modes at frequencies several times the sampling frequency. In addition, we present experimental results showing the determination of fundamental and harmonic vibration modes of a "drum" style dye-doped polymer membrane tautly mounted on a 12-inch circular hoop and excited with 30 Hz and 62 Hz sinusoidal acoustic waves. The projected laser dot pattern was generated by passing the beam from a pulsed Nd:YAG laser though a diffractive optical element, and the resulting fluorescence was imaged with three digital video cameras, all of which were synchronized with a pulse and delay generator. Although the video cameras are capable of 240 Hz frame rates, the laser's output was limited to 30 Hz and below. Consequently, aliasing techniques were used to allow the measurement of vibration modes up to 186 Hz with a Nyquist limit of less than 15 Hz.

INTRODUCTION

The term "Gossamer structure" is used in engineering to describe the general category of ultra-low-mass structures, which includes ultra-lightweight membrane space structures. [1] Gossamer structures are of interest to the space-structures community primarily because they are very light and can be packed into very small volumes, thereby reducing launch vehicle requirements and overall mission cost. [1] Both static shape and dynamic vibration measurements of transparent or highly reflective membranes has become a priority in the Gossamer space-structure community.

In the last few years, membrane space-structure technology has made significant advances and reached the point where high quality measurements of surface profile and dynamic behavior are required for further development. Photogrammetry is a technique that has proven to be a valuable tool for performing these measurements. [2-6] Photogrammetry is described as the science of determining three-dimensional measurements from multiple two-dimensional photographs though triangulation calculations, and requires high-contrast features on the structure being measured. [7,8]

Traditionally these high-contrast features are not naturally present on the structure, and therefore "targets" are created with adhesive retro-reflective tape. This tape is not ideally suited for membrane structures because it adds mass, alters stiffness, and can cause damage to the membrane, especially if removed. [6] Alternative methods of generating targets have been investigated but most have enjoyed limited success due to further complications arising because the polymers used for space structures are generally either highly transparent or highly reflective. [6] Recently we have overcome many of these problems with a new laser-induced fluorescence (LIF) approach, which has been demonstrated on a variety of highly transparent and reflective test structures for both static and dynamic photogrammetric measurements. [6,9-12] With this new technique, LIF is

utilized to create fluorescent targets by directing an array of laser beams at a polymer membrane that has had fluorescent dye added during the manufacturing process.

In this paper we introduce photogrammetry, review the laser-induced fluorescence photogrammetry (LIFP) technique and demonstrate how LIFP can be used to perform dynamic measurements of both highly transparent and highly reflective (aluminized) polymer membranes. Furthermore, we will show how a nanosecond-time-scale laser source and fluorescence lifetimes provide "snapshot" images that allows aliased measurements for the analysis of the structure's audio frequency vibrational modes above the Nyquist frequency (half the sampling frequency) of the imaging acquisition system.

Photogrammetry and traditional target generation

Photogrammetry is a technique for deriving a quantitative relationship between a 3D object and the 2D images acquired with still or video cameras [13]. The 3D shape of an object is obtained by "reverse engineering" two or more photographs using triangulation principles and algorithms. Photogrammetric principles were originally developed for the topographic mapping and surveying field, but in the last 20 years these techniques have evolved to support measurements of smaller objects in various industrial and research fields. This particular class of photogrammetry has become known as "close-range photogrammetry", and has been aided considerably by the development and common use digital imaging technology.

For accurate photogrammetric measurements, high-contrast surface features are required to appear in at least two photographic images. These high-contrast features are generally not naturally present and therefore must be artificially added, traditionally by painstakingly attaching retro-reflective targets to the object. These retro-reflective targets reflect light directly back to the camera when illuminated with a flash unit (for example), causing the targets to appear very bright in contrast to the background. Retro-reflective targets work exceptionally well and have very few drawbacks when used on rigid structures, but although they have been used on gossamer structures providing excellent results [2,4,5], they introduce several undesirable effects. The primary concerns are added mass and altered stiffness, which in turn alter and mask the true characteristics of the structures. In addition, the pattern of attached targets cannot be changed and the targets are very difficult or impossible to remove once affixed to the delicate membrane material. [6]

An alternative solution is to project the target pattern on the structure, thereby providing a completely non-contact measurement. [3,6] Projected dot patterns provide good results with diffuse surfaces because light is scattered in all directions, and the projected pattern can be viewed and photographed over a wide viewing angle. [3] However, gossamer structures are usually made form highly transparent or highly reflective material, resulting in very little diffusely scattered light. Consequently, exposure times as long as 30 seconds are required to obtain sufficient contrast images from white-light illuminated aluminized membranes. [6] These long exposure times prohibit the use of white-light projection for dynamic studies, and limit its application to static measurements. Furthermore, no measurements of white-light illuminated transparent membranes have been yet reported.

The appearance of "glints" or "hot-spots" further complicates photogrammetric observations of reflective structures, using either the retro-reflective or projected targets method. These hot-spots are areas of bright illumination on the image that is generated as a direct reflection from the camera flash or other unrelated source, such as room lights. Hot-spots reduce the contrast of targets, and in many cases completely occlude the targets in a localized region of the image, rendering these targets unusable. [5,9]

Laser-induced fluorescence target generation

Laser-induced fluorescence (LIF) is a process of inelastic scattering (where there is a change in wavelength) in which a portion of incident laser light is absorbed by a material (solid, liquid, or gas), and is then emitted at a longer wavelength. Many materials exhibit the phenomenon, but some are explicitly designed to utilize and optimize it. One example of such an optimized material is *laser dye*, which is usually dissolved in methanol and used as the optical gain medium in *dye lasers*.

For photogrammetric measurements of polymer membranes, generating targets with the use of fluorescence has several advantages. Firstly, fluorescence is emitted evenly in all directions giving a diffuse like appearance even if the material is transparent or reflective. Secondly, the projected excitation pattern and the emitted fluorescence can be spectrally separated (because there is a change in wavelength) with the use of optical filters blocking the laser wavelength, leading to the elimination of hot-spots and stray illumination light [9,11].

Polymers such as CP1™ and CP2™ used for ultra-lightweight space structures do not naturally exhibit high efficiency fluorescence. Therefore, in order to utilize LIF as a mechanism to generate photogrammetric targets, a fluorescent substance must be added to the polymer. For our experiments we added small quantities of Rhodamine 590 laser dye [Exciton, Dayton, Ohio] during the polymer's manufacturing process. When these dye-doped polymers are subjected to laser radiation at or near 532 nm, they fluoresce and emit light in all directions allowing high-contrast images to be obtained from almost any viewing angle.

To generate a fluorescing photogrammetry target pattern, an array of laser beams is generated with a diffractive optical element (DOE) [Stocker Yale, Montreal, Canada] and projected onto the structure being studied, as shown in Figure ~~Figure 1~~. The resulting fluorescing target pattern is then photographed though optical filters by two or more cameras and processed with photogrammetry software. Our previous research investigating the photo-physics of laser-dye-doped membranes has proven their suitability for photogrammetric target generation. [11] In particular, the fluorescence emission pattern was found to afford a wider viewing angle than diffuse scatter from white-light projected targets, and the laser-dye doped into the polymer was also found to have a substantial useful lifetime of more than 300,000 shots, or 3 hours of measurement. In addition, the fluorescence temporal decay time was found to be in the order of nanoseconds, which is several orders of magnitude faster than high-speed photography exposure times and well within the limits required for dynamic videogrammetry.

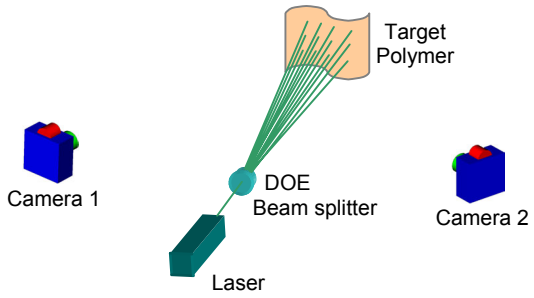

Figure 1 - Laser-induced fluorescence photogrammetry principle (camera filters not shown).

EXPERIMENT DESCRIPTION

Experimental Set-up

The experimental set-up is very simple and closely follows that described in Figure 1. A pulsed, frequency-doubled Nd:YAG laser [YQL-102, Laser Photonics Inc] producing approximately 10 mJ per pulse at 532 nm in 10 ns pulses with variable repetition rate up to 30 Hz was used as the excitation source. The laser beam was passed though a DOE to produce a 19-by-19 dot grid, which was projected onto the object. Images were recorded simultaneously with three Pulnix TM-7610 digital video cameras attached to a PC computer fitted with digital video acquisition cards [Bitflow, RUN-PCI-24M, Woburn, MA] and software. The laser pulse rate and video camera acquisition rate were controlled and synchronized with a Stanford Research Systems [Sunnyvale, California] pulse generator model DG535.

The article being studied is a 12-inch diameter CP1 polymer membrane doped with Rhodamine 590 laser dye manufactured by SRS Technologies [Huntsville, AL]. It is stretched over a hoop to provide near-uniform tension, and therefore exhibits "drum" like qualities and can easily be acoustically stimulated into vibrational modes. In the present experiment, this characteristic is utilized and membrane motion is excited with a loudspeaker driven by a signal generator [Model 23, Wavetek] placed behind the polymer. Two similar test articles were studied during these experiments, one transparent membrane and one highly reflective aluminized membrane. Figure 2 shows photographs of the experimental set-up and generated LIF targets. The first photograph shows the transparent polymer, loudspeaker, signal generator, and two of the three video cameras, while the second photograph shows a closer view of fluorescent photogrammetric targets generated on the aluminized polymer under laser excitation and viewed though a filter that blocks the laser's wavelength. For photogrammetric purposes, the background would normally not be visible in the second photographs and the target contrast would be higher. However, in this case the exposure setting was intentionally increased in order to show the background.

Unlike conventional imaging, the fluorescence intensity recorded on each acquired video frame is independent of exposure time setting if the laser pulse is timed to fall within the integration period. Consequently, it is advantageous to reduce the exposure time to the minimum possible setting, thereby rejecting as much background illumination as possible. Doing so allows operation of the LIF system in full room lighting without compromising target contrast. In our set-up, the exposure time could only be reduced to 1/4,000 of a second because of poor trigger synchronization between cameras. Even at this exposure setting, the laser and fluorescence pulse is still four orders of magnitude shorter than the cameras' shutters. Thus, the ambient light levels could potentially have been rejected by four more orders of magnitude using faster and better synchronized cameras. This was not necessary in the present experiment.

To find the polymer's natural frequency the signal generator was configured to drive the loudspeaker with a sine wave and was manually swept across the low audio range while the polymer was visually observed. Definite vibration modes were found at frequency settings of 30 Hz and 62 Hz. An attempt was then made to measure the polymer's displacement modes at these frequencies with videogrammetry. As mentioned previously, the limit of acquisition rate for the laser and video system is 30 Hz, which limits the maximum measurable bandwidth to 15 Hz as defined by the Nyquist criteria. Obviously attempting to directly measure displacements at 30 Hz and 62 Hz violate the Nyquest limit for the acquisition system, and is not possible.

However, the very short-pulsed nature of the laser system, and the comparable short fluorescence lifetime of the laser-dye provides the ability to obtain an almost instantaneous "snap-shot" of the polymers shape ultimately allowing aliased measurements of its vibration.

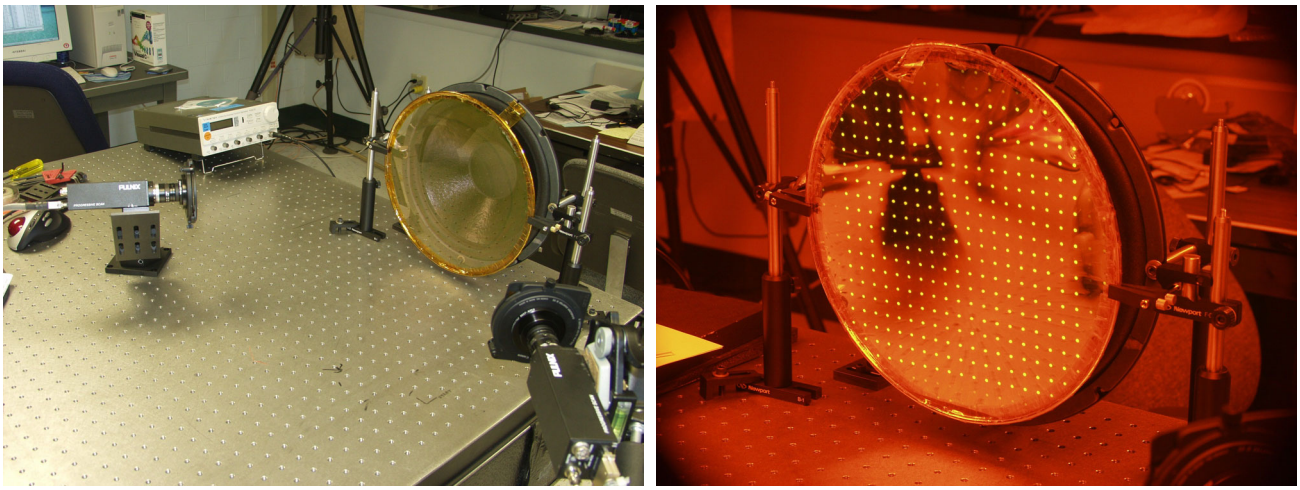

Figure 2 – Photographs of the experimental set-up with the transparent polymer (left) and the reflective aluminized polymer fluorescing under laser excitation viewed though the laser-blocking filter (right).

Aliasing Theory

According to the aliasing theorem, any signal of frequency above the Nyquist limit appears as an aliased signal at a lower frequency after sampling. The frequency of the aliased signal is the difference between the sampling frequency and the frequency of the input signal begin sampled, or for higher frequencies the difference between the closest integer multiple of the sampling frequency and the input signal frequency. Of course, for a given aliased frequency there are an endless number of candidate input frequencies that would also alias to the same frequency, and with this data alone the original input frequency cannot be positively identified. If however, another set of data were acquired at a different sampling rate, a different list of candidate frequencies would be produced. Only one of the candidate frequencies would be common to both lists (provided the two sampling frequencies are chosen carefully) and therefore the true input signal can be identified within resonable limits.

For example, if the 30 Hz vibration of the polymer was sampled by the laser and video system at 28 Hz, the aliased frequency would appear to be 2 Hz. Table 1 shows the list of the first 10 candidate input frequencies that would also alias to 2 Hz. If the experiment were performed again at a sampling rate of 29 Hz, the 30 Hz vibration would alias to 1 Hz, and the corresponding list of candidate input frequencies are also shown in table 1. By examining the two lists it can be seen that only one candidate input frequency is common to both lists, namely the correct input frequency of 30 Hz.

2 Hz alias at 28 Hz sampling	1 Hz alias at 29 Hz sampling	6 Hz alias at 24 Hz sampling
26	28	18
30	30	30
54	57	42
58	59	54
82	86	66
86	88	78
110	115	90
114	117	102
138	144	114
142	146	126

Table 1 – Lists of candidate input frequencies for a 2 Hz alias at 28 Hz sampling, a 1 Hz alias at 29 Hz sampling, and a 6 Hz alias at 24 Hz sampling frequencies. Note that the only common value for the 28 Hz and 29 Hz cases is a 30 Hz input frequency (double underlined), but there are two additional common values for the 28 Hz and 24 Hz cases (single underlined).

Although this technique appears to provide a unique solution, this is not actually the case. If the first two columns of Table 1 were extended to 55 entries, another common frequency of 782 Hz would be found. For this application it is if obvious that this solution is not sensible and the first solution is most probably correct. However, if the sampling frequencies were not chosen carefully, the ambiguity would be considerably more troublesome. An example of a poor choice of second sampling frequency is 24 Hz instead of 29 Hz, which is also shown in table 1, where three common frequencies (30, 54, and 114 Hz) would be found in the first 10 entries of table 1 alone.

In our application, we performed the experiment at the three different sampling frequencies 26.5 Hz, 28 Hz, and 29 Hz for additional redundancy. These sampling frequencies were carefully chosen prior to the experiment being performed to be sure that:

- there would be no ambiguity in determining the actual vibration frequency (as discussed above), and
- the fundamental and first two harmonics would not alias to the same frequencies.

The expected aliased frequencies for both the 30 Hz and 63 Hz vibration modes are listed in table 2.

Resonance frequency	Aliased frequency at sample rate 26.5 Hz	28 Hz	29 Hz
30 Hz fund.	3.5	2	1
30 Hz 2nd	7	4	2
30 Hz 3rd	12.5	6	3
62 Hz fund.	9	6	4
62 Hz 2nd	8.5	12	8
62 Hz 3rd	0.5	10	12

Table 2 – List of expected aliased frequencies for each vibration mode at each sampling rate. Note that for a given sample rate the aliased frequencies for each harmonic are different, and the aliased frequencies for a given harmonic are different for each sample rate.

DATA PROCESSING AND RESULTS

For each run of the experiment, 1000 frames of video data was acquired for each of the three cameras. These video sequences were processed using the Photomodeler software package [Eos Systems Inc., Vancouver BC, Canada]. Three-dimensional point data for every video frame was exported from Photomodeler™ and further processed with a Matlab [The MathWorks, Inc., Natick, MA] script. Because the coordinate system was defined during the photogrammetric processing to have the membrane in the x-y plane, only the z-axis data, or out-of-plane displacement is considered during further processing. The time sequence for each target was then individually multiplied with a Blackman window, padded with zeros, and Fast-Fourier Transformed (FFT), before a peak search was performed to find the frequency of the dominant displacement mode. The zero padding helped improve the precision of the peak search and provided a mechanism to ensure the same bin size of 5 mHz regardless of sampling rate. The aliased frequencies can clearly be identified in Figure 3, which graphs the average amplitude components of all targets for each of the sample frequencies at each vibration mode of the transparent polymer. Harmonics can also be seen, but appear at significantly lower amplitudes.

Tables 3a and 3b show the averaged measured frequencies for each case and the determined source frequency. For all measurements at 30 Hz excitation, the measured aliased frequencies match across all sample rates within one FFT bin width of 5 mHz. With 62 Hz excitation, the 2nd and 3rd harmonic measurements deviate slightly at different sample rates. This is probably due to the poor signal-to-noise (S/N) ratio caused by the very small displacements in these vibrational modes. In all cases, there is deviation of determined frequencies from the set excitation frequency probably because one of signal generators used for audio excitation or sample synchronization were not calibrated. For the purposes of this investigation, calibration errors are not important, and do not detract form the demonstration of the ability to measure membrane vibration above the Nyquist limit.

The average peak frequency was then used to determine the amplitude, and phase at that frequency for each target on the membrane from the original FFT data. Simple analysis of the spatial modes of the polymers was also performed by individually measuring the amplitude and phase of the previously identified dominant frequency for each of the projected targets. This data was then used to generate a surface plot of the displacement that shows the contribution from the dominant mode only. The surface plots for both 30 Hz and 62 Hz excitation frequencies of the fundamental, 2nd, and 3rd harmonics are shown in Figure 4, and are typical for this type of simple structure. For each of the plots in Figure 4, the best example was chosen from the selection of transparent or aluminized polymer, and the different sampling rates. There was little difference in the mode shapes for the fundamental frequency plots, with the exception of a slight increase in noise is some cases. The harmonic frequency plots shown in Figure 4 have a poor S/N ratio because of the small displacement in these modes, and hence poor S/N ratio in the original measured displacement data. Some of the other harmonic frequency plots not shown here were swamped with noise and the mode shape could not be determined.

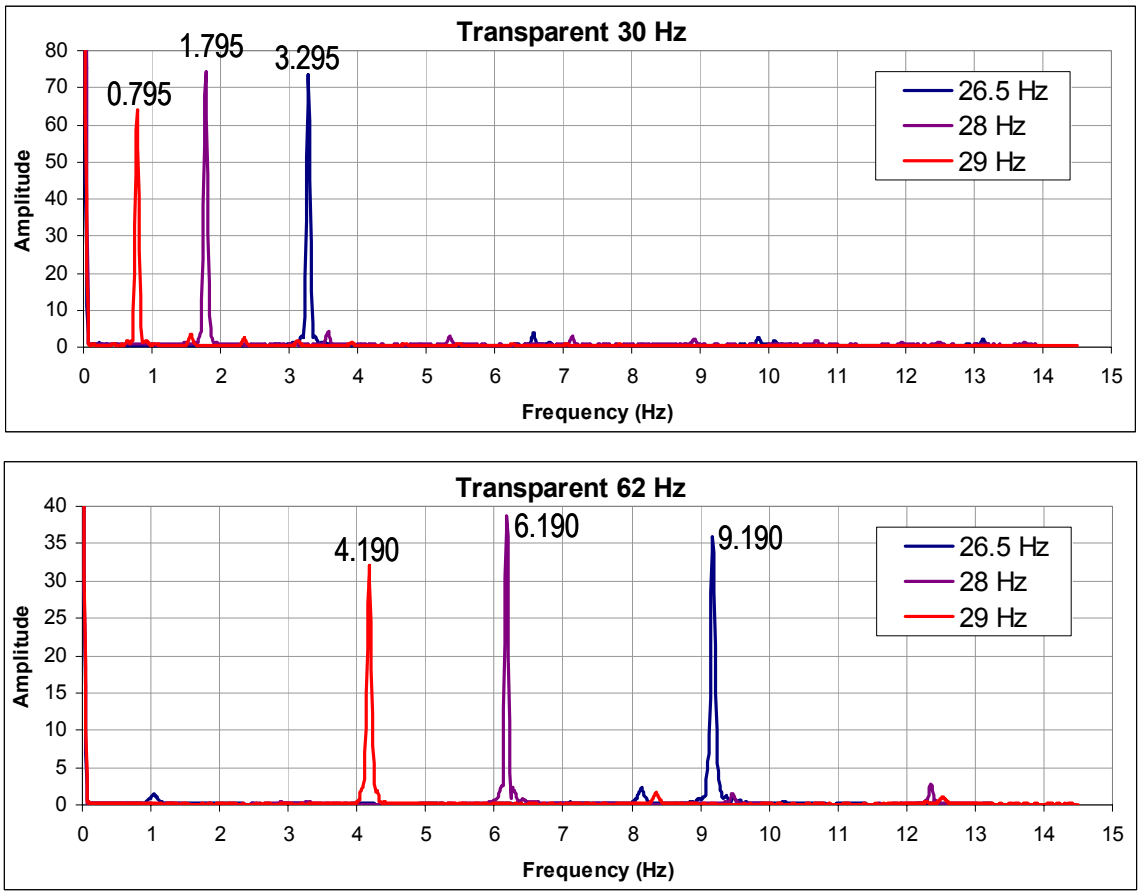

Figure 3 – Graphs of the out-of-plane displacement spectral content averaged across all measurement targets for the different sample rates in both 30 Hz and 62 Hz excitation frequencies.

The measurements presented here were performed with single-frequency audio excitation from the loudspeaker. However, this analysis method should also work satisfactorily with random excitation. If the structure exhibits a limited number of vibration modes, wide-band random excitation could be used and the actual frequency of the aliased vibration modes determined as described above. However, if too many modes are excited, it may not be possible to distinguish and correlate the aliased modes between measurements at different sampling rates. In this situation, the random excitation signal could be band limited to reduce the number of modes excited to a level where they could be adequately distinguished. At the extreme, the excitation signal bandwidth could be limited to approximately the value of the Nyquist frequency, resulting in no possible confusion of the original signal frequency because only one aliased band is excited and no two signals can alias to the same frequency. Scanning the band-limited random single across the whole spectrum could then cover the full bandwidth of random excitation.

Although we used laser-induced fluorescence as the target generation method in this experiment, these aliasing principles could also be used with traditional photogrammetric target generation techniques in other applications. For example, retro-reflective targets could be used with a video camera and synchronized strobe light if the strobe pulse width is sufficiently short compared to the vibration frequencies of interest. Additionally, we speculate that using two illumination and camera systems (running at different frame rates) at the same time could allow measurements of non-repeating single shot events provided care was taken to ensure these systems do not interfere with each other. Non-interference could be realized with techniques such as wavelength separation (different color illumination and camera filtering).

Table 3a

	30 Hz Resonance	Measured frequency (5 mHz FFT bins) 26.5Hz	28Hz	29Hz	Average
Transparent	Fundamental	3.295 **29.795**	1.795 **29.795**	0.795 **29.795**	**29.795 Hz**
	2nd Harmonic	6.575 **59.575**	3.575 **59.575**	1.575 **59.575**	**59.757 Hz**
	3rd harmonic	9.860 **89.360**	5.360 **89.360**	2.360 **89.360**	**89.360 Hz**
Aluminized	Fundamental	3.320 **29.820**	1.820 **29.820**	0.825 **29.825**	**29.822 Hz**
	2nd Harmonic	6.635 **59.635**	3.635 **59.635**	1.635 **59.635**	**59.635 Hz**
	3rd harmonic	9.945 **89.445**	5.445 **89.445**	2.450 **89.450**	**89.447 Hz**

Table 3b

	62 Hz Resonance	Measured frequency (5 mHz FFT bins) 26.5Hz	28Hz	29Hz	Average
Transparent	Fundamental	9.190 **62.190**	6.190 **62.190**	4.190 **62.190**	**62.190 Hz**
	2nd Harmonic	8.150 **124.350**	12.365 **124.365**	8.365 **124.365**	**124.360 Hz**
	3rd harmonic	1.050 **186.550**	9.475 **186.525**	12.540 **186.540**	**124.360 Hz**
Aluminized	Fundamental	9.200 **62.200**	6.200 **62.200**	4.200 **62.200**	**62.200 Hz**
	2nd Harmonic	8.130 **124.370**	12.395 **124.395**	8.390 **124.390**	**124.385 Hz**
	3rd harmonic	1.085 **186.585**	9.435 **186.565**	12.585 **186.585**	**186.578 Hz**

Tables 3a and 3b – Averaged peak frequencies for each excitation frequency, sample rate, polymer, and harmonic frequency. Aliased frequencies are shown in normal type, and determined actual frequencies are shown in bold type.

CONCLUSION

This paper reviewed the use of laser-induced fluorescence as a photo- and videogrammetric target generation method especially suitable for highly transparent and highly reflective membrane materials. We have also demonstrated that a short-pulse laser, in combination with a short-fluorescence-lifetime dye, effectively provides an instantaneous “snap-shot” of a moving membrane, regardless of camera integration time. More importantly however, it has been shown how aliased sampling (utilizing this “snap-shot” functionality) can be used to perform non-contact three-dimensional measurements of vibrational modes at frequencies in excess of the Nyquist limit of the imaging system. Specifically, vibration modes around 30 Hz and 62 Hz have been measured along with their 2nd and 3rd harmonics with a laser illumination and video acquisition system running at a maximum of 29 Hz. Furthermore, the original frequencies of these displacement modes have been determined despite them all being aliased into lower-frequency baseband. The major objective of the experiment was to demonstrate the capability of performing measurements above Nyquist limit. This objective has been achieved for single frequency excitation, and inferred for band-limited white-noise excitation.

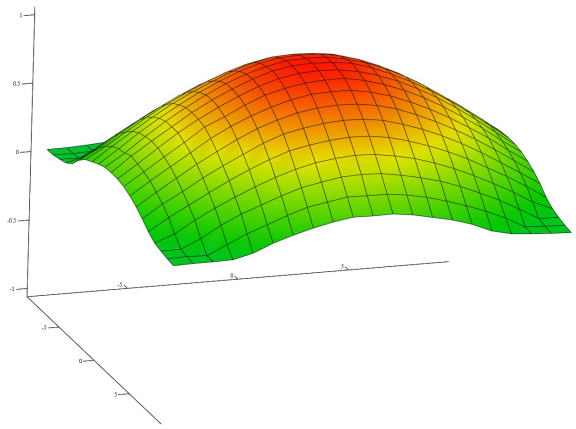

30 Hz Excitation, Fundamental
Aluminized polymer at 29 Hz sampling

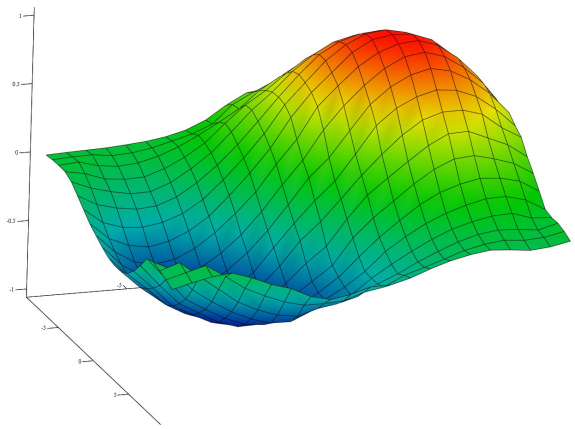

62 Hz Excitation Fundamental
Aluminized polymer at 29 Hz sampling

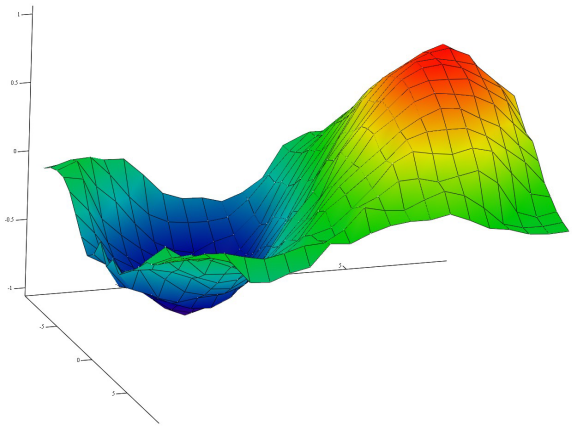

30 Hz Excitation, 2nd Harmonic
Aluminized polymer at 29 Hz sampling

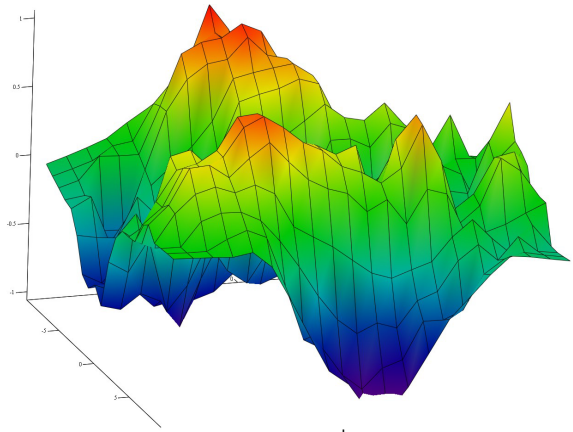

62 Hz Excitation, 2nd Harmonic
Transparent polymer at 28 Hz sampling

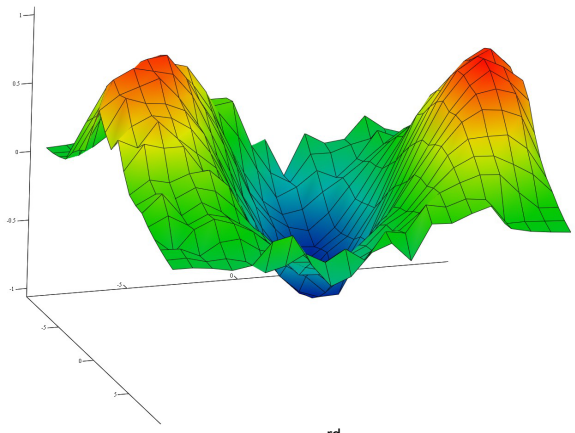

30 Hz Excitation, 3rd Harmonic
Aluminized polymer at 29 Hz sampling

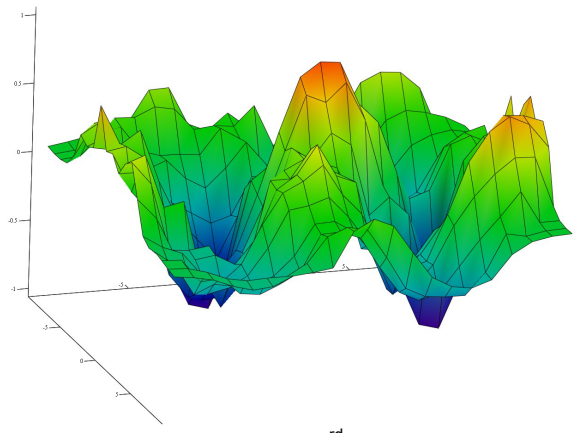

62 Hz Excitation, 3rd Harmonic
Transparent polymer at 29 Hz sampling

Figure 4 – Surface plots of the individual frequency contribution displacement mode shapes at the fundamental, 2nd, and 3rd harmonics (1st, 2nd, and 3rd rows respectively) for both 30 Hz (left column) and 62 Hz (right column) excitation. The flat potions of the plot at the corners are caused by missing data points falling outside the polymer and are purely an artifact of the plotting program.

REFERENCES

1 Chmielewski, A.B., "Overview of Gossamer Structures" in *Gossamer spacecraft: Membrane and inflatable structures technology for space applications, Vol. 191, Progress in Astronautics and Aeronautics*, Jenkins, C.H.M., ed. (AIAA, Reston, Virginia), pp. 1-33, 2001.

2 Pappa, R.S., Giersch, L.R., Quagliaroli, J.M., "Photogrammetry of a 5m inflatable space antenna with consumer-grade digital cameras," Experimental Techniques, Society for Experimental Mechanics, Vol. 25, pp. 21-29 (2001).

3 Jones, T. W. and Pappa, R. S., "Dot projection photogrammetric technique for shape measurements of aerospace test articles," AIAA Paper 2002-0532, 40th AIAA Aerospace Sciences Conference, January 2002.

4 Dharamsi, U.K., Evanchik, D.M., Blandino, J.R., "Comparing photogrammetry with a conventional displacement measurement technique on a square Kapton membrane," AIAA paper 2002-1258, 43rd AIAA Structures, Structural Dynamics, and Materials Conference, Denver, Colorado, 22-25 April 2002,.

5 Pappa, R.S., Jones, T.W., Black, J.T., Walford, A., Robson, S., and Shortis, M.R.. "Photogrammetry methodology development for gossamer spacecraft structures," AIAA Paper 2002-1375, 43rd AIAA Structures, Structural Dynamics, and Materials Conference, Denver, Colorado, 22-25 April 2002,.

6 Pappa, R.S., Black, J.T., Blandino, J.R., Jones, T.W., Danehy, P.M., and Dorrington, A.A., "Dot-projection photogrammetry and videogrammetry of gossamer space structures," AIAA Journal of Spacecraft and Rockets, Vol. 40, No. 6, pp. 858-867, 2003.

7 Mikhail E.M., Bethel J.S., and McGlone J.C., *Introduction to modern photogrammetry* (John Wiley and Sons, New York, 2001).

8 Gruen, A., "Development of digital methodology and systems" in *Close range photogrammetry and Machine Vision*, Atkinson, K.B., ed. (Whittles Publishing, Scotland, UK), pp. 78-104, 2001.

9 Dorrington, Adrian A., Jones, Thomas W., Danehy, Paul M., Pappa, Richard S., "Laser-induced fluorescence photogrammetry for dynamic characterization of transparent and aluminized membrane structures", AIAA Paper 2003-4798, 39th AIAA/ASME/SAE/ASEE Joint Propulsion Conference, Huntsville, Alabama, 20-23 July 2003.

10 Jones T.W., Dorrington A.A., Brittman P.L., Danehy P.M., "Laser induced fluorescence for photogrammetric measurement of transparent or reflective aerospace structures," 49th International Instrumentation Symposium, Orlando Florida, May 2003.

11 Dorrington A.A., Jones T.W., Danehy P.M., "Laser-induced fluorescence photogrammetry for profiling gossamer space structures," Conference on Lasers and Electro-optics 2003, Baltimore, Maryland, June 2003.

12 Jones, Thomas W., Dorrington, Adrian. A., Shortis, Mark R., and Hendricks, Aron R., "Validation of laser-induced fluorescent photogrammetric targets on membrane structures", AIAA Paper 2004-1663, Accepted for the 45th AIAA/ASME/ASCE/AHS/ASC Structures, Structural Dynamics & Materials Conference, Palm Springs, California, 19-22 April 2004.

13 Burner A.W., Liu T., "Videogrammetric model deformation measurement technique," Journal of Aircraft, Vol. 38, No. 4, pp. 745-754, 2001.